NASA TN D-1707

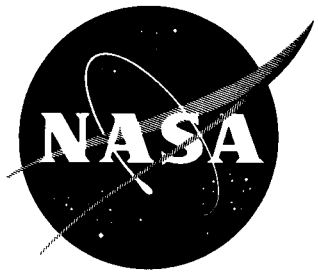

TECHNICAL NOTE

D-1707

PRELIMINARY INVESTIGATION OF MELTING, EXTRUDING, AND MECHANICAL PROPERTIES OF ELECTRON-BEAM-MELTED TUNGSTEN

By Walter R. Witzke, Earl C. Sutherland, and Gordon K. Watson

Lewis Research Center
Cleveland, Ohio

NATIONAL AERONAUTICS AND SPACE ADMINISTRATION
WASHINGTON

May 1963

NATIONAL AERONAUTICS AND SPACE ADMINISTRATION

TECHNICAL NOTE D-1707

PRELIMINARY INVESTIGATION OF MELTING, EXTRUDING, AND MECHNICAL PROPERTIES OF ELECTRON-BEAM-MELTED TUNGSTEN

By Walter R. Witzke, Earl C. Sutherland, and Gordon K. Watson

SUMMARY

Commercially sintered and arc-melted tungsten materials were melted and remelted in a 150-kilowatt electron-beam furnace to form ingots $2\frac{1}{4}$ inches in diameter and ranging from 7 to 27 inches long. Remelting produced an improved surface over that of the first melting. During initial melting, purification of the tungsten was evidenced by outgassing of the melt. Chemical analysis of the melted tungsten provided primarily qualitative indication of increased purity.

Most of the billets machined from the electron-beam-melted ingots were extruded in a Dynapak press, and one was extruded in a 750-ton hydraulic extrusion press. Successful extrusions of 8 to 1 and of 10 to 1 reductions were obtained at 3000° or at 3200° F. The microstructures of the extruded bars indicated a predominantly hot-worked structure. The surface appearance of the low-velocity extrusion bars was good, whereas the surfaces of those bars obtained by high-velocity extrusion exhibited "raisin-type" defects.

Tensile properties of extruded electron-beam-melted tungsten and of commercially pure powder metallurgy tungsten recrystallized to the same grain size (0.05 mm) were compared. The electron-beam-melted tungsten with its higher purity had approximately 12 percent lower ultimate tensile strength than the powder metallurgy tungsten at all temperatures from 70° to 3900° F. Contrary to expectations, the ductile-to-brittle transition temperature of the electron-beam-melted tungsten was higher than that of powder metallurgy tungsten of comparable grain size. The recrystallization behavior of wrought electron-beam-melted tungsten was studied. Material swaged 70 percent after extrusion had a recrystallization temperature of 2120° F, about 600° to 700° F lower than has been observed for powder metallurgy tungsten after equivalent working. This low recrystallization temperature is regarded as evidence of the higher purity of electron-beam-melted tungsten.

INTRODUCTION

During the past few years, the needs of a rapidly growing aerospace science

have expanded the interest in refractory metals, tungsten, tantalum, molybdenum, and columbium, as potential high-temperature structural materials. These metals have been produced for many years by powder metallurgy techniques, but this method usually limits the size, the density, or the purity of the resulting ingot. In recent years, vacuum melting of the refractory metals has been investigated extensively (refs. 1 to 4), and vacuum arc-melted metals and alloys are currently produced commercially. The NASA Lewis Research Center has utilized arc melting extensively in studies of tungsten and its alloys (ref. 5). Electron-beam melting has been studied less extensively, but it is also practiced commercially for the production of high-purity columbium, tantalum, and their alloys (ref. 6).

Electron-beam melting offers a method of slow melting under a high vacuum; thus many contaminants normally associated with the refractory metals are removed. As has been noted with other body-centered cubic metals, the ductile-to-brittle transition temperature of tungsten tends to be increased by the presence of interstitial impurities (ref. 7). For tungsten of commercial purity produced by powder metallurgy techniques, the ductile-to-brittle transition temperature in tension is well above room temperature, frequently as high as 600° to 800° F for recrystallized material. Therefore, electron-beam melting is of considerable interest as a method of purifying and thus of improving the ductility of this metal. Indeed, single crystals of tungsten prepared by zone melting in vacuum by use of electron-beam heating have been shown to be ductile by bend tests at room temperature (refs. 8 and 9). It has not been determined, however, whether the zone-melted tungsten is less brittle primarily because purity is increased or because it is a single crystal. Additional study is required with polycrystalline tungsten of the same purity as the single crystals to resolve this point. A survey of the literature indicated little information on the preparation or properties of polycrystalline tungsten produced by electron-beam melting (ref. 10), although "grain-refined electron-beam-melted tungsten" is now available from one commercial producer (ref. 11). The investigation described herein was undertaken at the NASA Lewis Research Center to examine the electron-beam melting of tungsten in vacuum, to observe the characteristics of this material on extrusion, and to determine the mechanical properties of the extruded electron-beam-melted tungsten. Ductile-to-brittle transition temperature was examined for possible improvement as a result of electron-beam melting.

The preliminary results of this investigation are reported herein. Two types of tungsten feed ingots were melted in a 150-kilowatt electron-beam furnace. Tungsten billets machined and ground from the electron-beam-melted ingots were extruded in both high-velocity (Dynapak) and comparatively low-velocity (hydraulic) extrusion presses. Tensile specimens were cut and ground from the extruded tungsten. The mechanical properties of these electron-beam-melted specimens were determined from room temperature to 3900° F. These data were compared with those of commercial powder metallurgy tungsten annealed to the same grain size.

ELECTRON-BEAM MELTING

Electron-Beam Furnace

Melting was performed in a 150-kilowatt commercial electron-beam furnace.

This unit is capable of melting and casting a tungsten ingot of $2\frac{1}{4}$-inch diameter by 28-inch maximum length at a chamber pressure of 10^{-5} millimeter of mercury. The vacuum system consists of a 32-inch oil diffusion pump rated at 25,000 liters per second at 10^{-4} millimeter of mercury, backed by a 1250-cubic-feet-per-minute mechanical booster pump and a 140-cubic-feet-per-minute mechanical roughing pump. The essential features of the electron-beam-melting equipment within the vacuum chamber are shown in figure 1.

Melting of Tungsten

The melting operation can be described briefly as follows: Electrons are emitted from a heated filament in the ring-shaped "electron gun." Because of a high voltage (10 kv) imposed on the electron gun, the electrons travel at a high velocity and are effectively focused on the grounded tungsten ingot. The kinetic energy of the electrons, on impact, is converted to heat energy and, in sufficient quantity, causes melting of the tungsten. Once a molten pool of tungsten has been formed on the starter piece in the water-cooled crucible, the tungsten feed rod is lowered into the gun. Electrons bombard the end of the feed rod, melt the tip, and cause drops of tungsten to fall into the molten pool. As the tungsten solidifies in the crucible, the formed ingot is lowered; a molten pool of tungsten is maintained at a constant level at the top of the crucible.

A more detailed description of this type of furnace and its operation is given in reference 6. A description and discussion on the ring-type and other electron guns are presented in reference 12.

Because of the high melting point of tungsten and its high thermal conductivity, high power levels are required for melting. Power densities ranging from 22 to 33 kilowatts per square inch of ingot cross-sectional area were used for drip melting. The higher power density is about the same as that used in the arc melting of tungsten (ref. 5).

Three tungsten ingots were melted for this study. The ingots were approximately $2\frac{1}{4}$ inches in diameter; their lengths were about 7, 21, and 27 inches long. Two types of feed ingots were used: (a) commercially available sintered rods approximately 1 inch in diameter and (b) vacuum arc-melted ingots approximately 2 inches in diameter. Each ingot was melted at least twice. Purification was the primary aim of the first melt; whereas, the second melt was performed to obtain a good surface on the ingot. There was a great difference in the melting characteristics of the materials during the first melt. The sintered rods exhibited considerable outgassing during the initial melt, as evidenced both by the frequent off-on operation of the electric power supply and by the "spitting" of many small bits of glowing material, molten tungsten, from the feed rod. The power supply automatically turned off for a fraction of a second whenever the pressure became too high within the space around the gun. In contrast, the arc-melted feed ingot melted quietly with little indication of degassing. Remelts of ingots electron-beam melted from both types of materials also melted quietly with comparatively rapid dripping.

Melting rates during electron-beam melting are strongly dependent on the amount of outgassing encountered. Average melting rates of the three ingots of this investigation are shown in table I. During the first electron-beam melt, rates ranged from about 3 pounds per hour for the sintered feed rods to $7\frac{1}{2}$ pounds per hour for the arc-melted material. During remelting, rates as high as 25 pounds per hour were achieved. These rates are very much lower than in vacuum arc melting, where melting rates from 1 to 5 pounds per minute (60 to 300 lb/hr) are typically encountered for ingots of the same size. Thus, there is considerably more opportunity for purification during electron-beam melting than during arc melting. It also should be noted that more opportunity for purification results from exposing the melt to the chamber pressure by melting at the top of the crucible rather than near the bottom of the crucible as is normally practiced in arc melting.

Chemical Analysis

Chemical analysis of the starting materials, of a typical electron-beam-melted ingot after two melts, and of a typical arc-melted ingot (average of five single melts) are shown in table II. The metallic impurities were determined by an independent laboratory using emission spectrographic analysis. Nitrogen analysis was carried out by an independent laboratory using the Kjeldahl method. The analyses for carbon, oxygen, and hydrogen were made at the Lewis Research Center. Carbon was determined by the Leco conductometric method, and oxygen and hydrogen were determined by vacuum extraction. The spectrographic analysis of the arc-melted tungsten was made at an earlier date than were either the analyses of the sintered or of the electron-beam-melted tungsten. During this time interval, improved techniques caused lowering of the detection limits. The carbon determinations had the same value for precision and for accuracy, namely ±10 percent at 9 parts per million (ppm) (ref. 13). The oxygen determinations had a precision of ±20 percent at 5 ppm. Although limits were not indicated by the independent laboratory, nitrogen analyses by the Kjeldahl method have been reported to have a precision of ±5 percent at 15 ppm (ref. 14). No limits on the accuracy of the oxygen or nitrogen analyses were available. No attempt was made to establish the homogeneity of the ingots analyzed.

The chemical analyses of both the commercial high-purity sintered and the arc-melted feed stocks are quite similar, although, as stated previously, there was a great difference in melting characteristics during the first melt. Comparison of the chemical analyses of the electron-beam-melted tungsten and those of the sintered and arc-melted tungsten feed stocks show only minor differences in purity content. The largest difference to be noted is 13 ppm as indicated for iron content. Since most impurities in these materials are present in amounts corresponding closely to their limits of detection, such analyses do not give a strictly quantitative measure of the degree of purification attained. Further indication of the degree of purification achieved by electron-beam melting can be obtained by comparing the interstitial content. In order to determine whether additional purification (or contamination) would result from repeated melting, one ingot was melted a total of five times, and an attempt was made to follow the interstitial levels after the second, fourth, and fifth melts. The results are shown in the following table:

Electron-beam melt	Interstitial element, ppm by weight			
	Oxygen	Hydrogen	Nitrogen	Carbon
2nd	3	<1	10	5
4th	2	<1	3	7
5th	3	<1	7	10

There is no substantial evidence of further purification resulting from remelting more than once. Carbon analyses generally indicate contents of 5 and 6 ppm in initial melts and first remelts (unpublished data obtained at Lewis). The slight rise in carbon content shown here after additional remelts may have resulted from contamination by diffusion pump oil.

Ingot Characteristics

The Vickers hardness of the electron-beam-melted tungsten ingots averaged about 350 (10-kg load) and ranged from 328 to 385. These values are similar to those obtained on vacuum arc-melted tungsten ingots in reference 5. Measurements of hardness were made on large grains of different orientation in an electron-beam-melted ingot. These measurements showed little or no dependence of hardness on orientation; that is, the range of values for differently oriented grains was about the same as the range of values for many impressions within a single grain.

The variations in surface texture of electron-beam-melted tungsten ingots are shown in figure 2(a). In the present state of the art, it is not unusual to obtain tungsten ingot surfaces with wrinkles as deep as 1/4 inch; the wrinkles are not uniform and their depths vary. The surface of the electron-beam-melted tungsten ingot after a single melt is very irregular. Remelting improves the surface quality of the ingot; however, additional remelts are not necessarily better in surface quality. The gradual deterioration of the crucible surface is believed responsible for some of the poor ingot surfaces. Also, a limited power supply prevented substantial superheating of the melt. It is probable that the lack of adequate superheating caused most of the surface defects.

Unfortunately, the melting of $2\frac{1}{4}$-inch-diameter tungsten ingots required all the power available to the furnace. The lack of power limited the ability to cast tungsten with surfaces as smooth as those cast from columbium (fig. 2(b)).

Electron-beam ingots are characterized by the large size and columnar nature of their grains (fig. 3). The grains, from 1/8 to 1/2 inch across and often several inches long, are considerably larger than those in arc-melted ingots (ref. 15). The large grain size of the tungsten ingots may be indirect evidence of their purity, for it suggests that few impurities were present to act as nucleation sites for new grains during freezing of the molten metal. The orientation of the grains in as-cast ingots appears to be random as determined by X-ray diffraction techniques (fig. 4).

Despite the high purity of electron-beam-melted tungsten indicated by the chemical analysis, the ingots are brittle at room temperature and little energy is required to initiate and to propagate intergranular fractures. This brittleness is illustrated in figure 5, which shows a fractured slice of tungsten. The fracture occurred when an attempt was made to cut the slice from a tungsten ingot. Although the brittleness of tungsten is frequently suggested as associated with segregation of impurities to grain boundaries (ref. 7), photomicrographs of the electron-beam-melted tungsten did not reveal the presence of any visible impurity phases in the grain boundaries (fig. 6). Impurities, however, could be present at the grain boundaries in concentration levels below their solubility limits in tungsten. Fractographs, typical for the three ingots examined here, are shown in figure 7. The grain boundary surfaces appear to be relatively clear although a few defects suggestive of microporosity are present.

EXTRUSION OF ELECTRON-BEAM-MELTED TUNGSTEN

For this investigation, 10 billets machined from the electron-beam-melted ingots were extruded, one in a 750-ton hydraulic extrusion press at a commercial laboratory and nine in a Dynapak extrusion pressure at Lewis. The preparation and inspection of the extrusion billets as well as their extrusion characteristics are described in the following sections.

Preparation and Inspection of Extrusion Billets

In preparing the extrusion billets, the tungsten ingots were usually rough machined to within 0.070 inch of the finish diameter. Grinding to final diameter completed the operation. Because of the poor adherence between grains, a number of grains were often pulled out of the billet surface during the rough machining and, to a lesser extent, during grinding.

After machining, the extrusion billets were inspected both by ultrasonic and dye-penetrant techniques. Ultrasonic inspection of the tungsten billets indicated the presence of possible cracks and some minute porosity.

Dye-penetrant tests on the extrusion billets revealed the presence of cracks along the grain boundaries at the ground surface (fig. 8). These flaws were most common in all billets on the transverse surfaces and were probably grinding cracks produced in the cutoff and surface grinding operations. In general, these defects appeared to be quite shallow and were not deemed serious enough to warrant rejection of the extrusion billet. The fact that the cracks were invariably intergranular emphasized the poor adherence between tungsten grains. Examination of the extruded bars failed to indicate any correlation between the flaws detected by ultrasonic and dye-penetrant inspection and the appearance of the extruded bar.

The billet extruded in the 750-ton hydraulic press was ground to a 2.060-inch diameter with a 120°-angle nose that tapered to approximately a 3/4-inch diameter. Billets for the Dynapak extrusion press had a 1.70-inch diameter and a 120° included angle on the nose and tapered to approximately a 1/2-inch diameter.

Extrusion Procedure

The billet extruded in the 750-ton hydraulic press was heated in an induction furnace under a flowing argon atmosphere. The temperature of the billet was measured by means of an optical pyrometer. After it was heated, the billet was placed in the extrusion press and forced through an alumina-coated steel die having approximately a 120° included angle. A Corning 7740 glass pad provided lubrication ahead of the billet.

Figure 9 shows a sectional view of the Dynapak extrusion press with the billet in position. Heating of the extrusion billet was carried out in an induction coil positioned around the billet and in line with the punch and the die. A plastic bag surrounding this coil permitted an inert atmosphere of argon to be maintained around the heated billet. A thermocouple inserted in a hole in the nose of the billet provided an accurate measure of the billet temperature prior to extrusion. This arrangement for heating the billet while in position for extrusion results in virtually instantaneous transfer time and in practically no loss in billet temperature. All dies used had openings with 120° included angles. As indicated in table III, the die coatings differed; some dies had no coatings and some had alumina or Corning 0010 glass coatings. The lubricants included Corning 7900 or 7740 glass as well as solid copper in the form of a nose pad.

Extrusion Results

The extrusion data for the electron-beam-melted tungsten billets are presented in table III. Most of these extrusions were made at 3000° or 3200° F and at reduction ratios of 8 and 10. The average Vickers hardness of the tungsten extrusions was approximately 360, very similar to that obtained for the as-cast electron-beam-melted tungsten. Figure 10 shows typical microstructures of the extruded bars. Examination of the microstructures of the extruded bars indicated a predominantly hot-worked structure; that is, the structure had been almost completely recrystallized during the extrusion. The grain size of the extrusions varied from bar to bar and was frequently nonuniform within each bar.

Photographs of tungsten extrusions of reduction ratios of 8 and 10 produced on the high-velocity press (Dynapak) are shown in figures 11(a) and (b), respectively. In general, the extrusions were comparatively good with only minor nose and tail cracking. Some difficulty was experienced in providing adequate lubrication for the electron-beam-melted billets during the extrusion process. This factor may have been responsible for the raisin-type defects found on the surface of the electron-beam-melted tungsten extrusions (figs. 11(a) and (b)). In comparison with work done previously at Lewis, the surface appearance of high-velocity extrusions of electron-beam-melted tungsten was slightly poorer than arc-melted tungsten, whereas, powder metallurgy extrusions of tungsten made under similar conditions generally had the least desirable surface appearance.

A comparison can be made between the electron-beam-melted and arc-melted tungsten extrusions formed in the low-velocity extrusion press. The electron-beam-melted tungsten billet extruded with equal or greater ease, as indicated by breakthrough pressure, than two arc-melted tungsten billets extruded under simi-

lar conditions (unpublished data obtained at Lewis). The breakthrough pressure was 137,600 psi for the electron-beam-melted material and 142,000 and 157,000 psi for the arc-melted material. The surface appearance of the electron-beam-melted tungsten extrusion was good; it was equal to that of arc-cast tungsten extrusions (fig. 12). Although only a few extrusions were made, it would appear that the surface of the extrusion made with the hydraulic press was better than those surfaces of the extrusions made with the Dynapak press.

MECHANICAL PROPERTIES OF WROUGHT ELECTRON-BEAM-MELTED TUNGSTEN

Mechanical properties of the extruded electron-beam-melted tungsten before and after swaging were determined. For comparative purposes, properties of swaged and recrystallized commercial tungsten bar stock prepared by powder metallurgy techniques were also determined. This work is described in the following sections.

Materials

Extrusions from all three ingots (EB10, EB15, EB20) were used to obtain mechanical properties both before and after swaging. A portion of the extruded bar from ingot EB15 was swaged from a nominal 3/4-inch diameter to approximately 3/8-inch diameter (70-percent reduction in area) at temperatures from 2200° to 2400° F. Small pieces of extrusions from tungsten ingots EB10 and EB20 were swaged in a similar manner to approximately 3/8 inch in diameter. Because of their smaller initial diameter, however, only about a 60-percent reduction in area resulted. The resulting microstructure of the swaged tungsten (ingot EB15, 70-percent cold work) is shown in figure 13 and may be compared with that of the as-extruded structures in figure 10.

Swaged commercial powder metallurgy tungsten rod of 3/8-inch diameter was also used to obtain comparative data. After machining, test specimens of this material were annealed 1 hour at 4200° F in order to produce a recrystallized structure similar to that of the as-extruded electron-beam-melted rod. The grain-size effect was thereby eliminated when the powder metallurgy material was compared with at least one of the as-extruded rods (EB15). The grain sizes of the materials were as follows:

Tungsten material	Average grain diameter, mm
EB10 extrusion	0.04
EB15 extrusion	.05
EB20 extrusion	.10
Annealed powder metallurgy rod	.05

It is recognized that the annealing treatment of the powder metallurgy tungsten at 4200° F produced an average grain size comparable to that of the extruded electron-beam-melted tungsten; however, it is not known what other changes may have occurred during the annealing treatment.

Test Procedure

Tensile tests with all the materials previously described were performed with equipment and test techniques similar to those described in reference 16. Tensile specimens were of the button-head type shown in figure 14. Except for room temperature runs, all the tests were conducted under vacuum conditions. Crosshead speeds were 0.005 inch per minute to approximately 0.2-percent yield and 0.05 inch per minute from yield to fracture.

The recrystallization behavior of electron-beam-melted tungsten was examined by annealing rods prepared by swaging (at 2200° F) the extruded bar from ingot EB15. Small sections of the as-swaged rod were heat-treated in a vacuum for 1 hour at several temperatures. After this treatment, they were sectioned longitudinally and examined metallographically and the Vickers hardness determined with a 10-kilogram load.

TEST RESULTS

Results of the tensile tests of extruded bars from each billet are tabulated in table IV. Table IV includes data on swaged samples of the extruded bars. The results of tensile tests on the recrystallized powder metallurgy tungsten rod are listed in table V. All these results are shown graphically in figures 15 to 19. Hardness data are tabulated in table VI and plotted in figure 20. Photomicrographs of fractured tensile specimens are shown in figure 21.

Effect of Temperature on Tensile Strength

The yield and the ultimate strengths of extruded electron-beam-melted tungsten at temperatures up to about 3900° F are shown in figure 15. Data from material from all three ingots appears to be on a single curve. Thus, there seems to be no significant correlation of tensile strength with the melting procedure employed in this investigation. Inasmuch as a significant difference occurred in the microstructure (grain-diameter range, 0.04 to 0.10 mm) of extruded bars from the different ingots, high-temperature strength also appears to be comparatively insensitive to the variation in grain size represented here.

Comparison of the data from the as-extruded electron-beam-melted tungsten with that for recrystallized powder metallurgy rod of comparable grain size (fig. 16) indicates that the powder metallurgy tungsten possessed about 12 percent higher strength at all temperatures investigated. The probable higher impurity content of the powder metallurgy tungsten is considered responsible for its higher strength.

As indicated in figure 17, swaging at 2200° to 2400° F after extrusion sig-

nificantly improves strength (particularly yield strength) at temperatures below 2500° F. For example, at 800° F the tensile strengths are 44,000 psi for as-extruded material and 60,100 psi after 60-percent cold work by swaging; yield strengths are 15,000 and 56,500 psi, respectively. As the test temperature approaches the recrystallization temperature, however, the effects of swaging tend to become nullified; that is, at 2500° F both materials have an ultimate tensile strength of approximately 18,000 psi, and the swaged material has a yield strength of 6700 as compared with 4700 psi for as-extruded metal. At temperatures above 3000° F they have the same properties.

Ductile-to-Brittle Transition Temperature

It has been thought that tungsten produced by electron-beam melting might be significantly more ductile than powder metallurgy tungsten as a result of its probable higher purity; thus, it should exhibit a lower ductile-to-brittle transition temperature. In figure 18, ductility (as measured by reduction of area in a tensile test) is shown for the transition-temperature range for specimens from the extruded bars of the three electron-beam-melted tungsten ingots and for the recrystallized swaged powder metallurgy material. The transition temperature is defined arbitrarily as the temperature at which the material exhibits 50-percent reduction in area. The various materials have the following transition temperatures:

Ingot	Number of electron-beam melts	Average grain diameter, mm	Transition temperature, °F
EB10	2	0.04	1090
EB15	5	.05	790
EB20	2	.10	940
Powder metallurgy rod	--	.05	640

Because of the limited amount of data, these transition temperatures are only approximate but they do indicate generally that the expectation of lower transition temperature for the electron-beam-melted material is not realized. Indeed, in its "normal" fine-grained condition, powder metallurgy tungsten usually exhibits a transition temperature of about 400° F (ref. 17), which is much lower than that of the electron-beam-melted tungsten investigated in this study. Other experiments with recrystallized wires drawn from powder metallurgy tungsten rod and from zone-refined tungsten rod indicated that the ductile-to-brittle transition temperature of the zone-refined wire is lower than that of the powder metallurgy wire of comparable grain size (ref. 18). The cause of the unanticipated high transition temperature in this investigation is undetermined, but it may be related to the greater variation of grain size in the extruded electron-beam-melted tungsten compared with the recrystallized powder metallurgy tungsten.

Other factors such as differences in substructure, prior working history, etc. may also be involved.

Since the transition temperature of tungsten is usually observed to decrease with increasing amounts of cold work, it was of interest to investigate the extent to which the transition temperature of electron-beam-melted tungsten could be lowered by a moderate amount of cold work. The results of tensile tests of material swaged from the extrusions of the three ingots are shown in table IV. The ductilities of extruded and of extruded plus swaged material (about 70-percent cold work) from one ingot (EB15) are compared in figure 19. Although the data are few, the transition temperature appears to have been lowered from 800° to about 500° F by this working operation.

High-Temperature Ductility and Fracture Characteristics of Electron-Beam-Melted Tungsten

In previous studies (refs. 19 and 20), it has been reported that arc-melted tungsten exhibits considerably more tensile ductility (as measured by reduction of area) at temperatures of about 3000° F than does powder metallurgy material. It has been speculated that this is an indication of the higher purity of the arc-melted material. In this respect, electron-beam-melted tungsten behaves very similarly to arc-melted tungsten in that all the tensile specimens from the extruded bars necked to virtual points at 2500° F or above and yielded a reduction in area in excess of 99 percent. In contrast, the powder metallurgy tungsten (recrystallized to a grain size comparable to the electron-beam-melted tungsten) showed a decrease in ductility in the 2500° to 3500° F range (table V).

Total elongation values tended to be erratic, but uniform elongation (elongation up to maximum load) was more consistent as indicated by plots (not shown) of the tabulated data. In general, little difference existed between the values of uniform elongation for specimens from the different ingots of electron-beam-melted tungsten (table IV). For the most part, uniform elongation values for the electron-beam-melted tungsten were somewhat higher than corresponding values for powder metallurgy tungsten at corresponding temperatures.

Recrystallization Study

The swaged extrusion of ingot EB15, which had five melts, was examined for its recrystallization temperature. The recrystallization behavior of the other two ingots was not determined. The swaged material, which had 70-percent cold work, was annealed for 1 hour at various temperatures. The results of hardness measurements made on the annealed specimens are tabulated in table VI and plotted in figure 20. With two-thirds of the total decrease in hardness and at least 50 percent of the recrystallized grain structure used as the criterion for the recrystallization temperature, it is determined to be 2120° F for the swaged rod from ingot EB15. This is unusually low for tungsten that has received only a 70-percent reduction by swaging, about 600° to 700° F lower than has been observed for powder metallurgy tungsten after equivalent working.

Metallographic Studies of Tensile Test Fractures

Photomicrographs of typical microstructures near the fracture region of the as-extruded electron-beam-melted tungsten specimens (EB10) are shown in figure 21. At the lowest test temperature (505° F), the fracture appears to be predominantly intergranular. Since the specimen fractured below the yield point, there is no evidence of plastic deformation. For the 980° F test temperature (just below the transition temperature), considerable deformation of the grains occurred prior to failure (fig. 21(b)). The fracture is primarily transgranular.

The fracture at 2000° F (fig. 21(c)) shows the typical microstructure of tungsten that has undergone a very high degree of plastic deformation; the fibrous grains end in a point fracture.

The fracture at 2500° F (fig. 21(d)) shows the microstructure to be virtually recrystallized. The material is very ductile, and the fracture is transgranular. The irregular grain size and shape indicate that the temperature is just over that required for recrystallization to occur.

At 3000° F (fig. 21(e)), the grain size at the fracture has become more equiaxed and considerable grain growth has taken place. The fracture remains transgranular.

At 3500° F (fig. 21(f)), fracture represents the high-temperature tensile break of a single crystal that has grown across the specimen diameter under the applied stress. This fracture demonstrates the very high degree of ductility found in high-purity tungsten at these temperatures.

SUMMARY OF RESULTS

A preliminary study was made to evaluate the melting characteristics, the extrudability, and the mechanical properties of extruded electron-beam-melted tungsten. The results of this study are as follows:

1. Electron-beam-melting techniques were used to provide tungsten ingots suitable for extrusion. Remelting the electron-beam-melted tungsten ingots gave an improved surface finish.

2. Outgassing of the melt, lower recrystallization temperature of the extruded and swaged electron-beam-melted tungsten, and lower tensile and yield strengths provided the principal evidences of increased purity in the electron-beam-melted product. Chemical analyses provided primarily qualitative indications of increased purity. Despite their apparent high purity, electron-beam-melted ingots were very fragile; intergranular fracture and grain "pull-out" were common defects.

3. Electron-beam-melted billets were extruded successfully by both high- and low-velocity extrusion processes at temperatures above 3000° F with reduction ratios of 8 and 10. The microstructures of the extruded bars indicated a predominantly hot-worked structure.

4. The ductile-to-brittle-transition temperature of the wrought electron-beam-melted tungsten, contrary to expectations, was higher than that of powder metallurgy tungsten of a comparable grain size.

5. The extruded electron-beam-melted tungsten had a lower tensile strength than powder metallurgy tungsten of the same grain size over the entire temperature range from 500° to 3900° F and a higher ductility in the high temperature range from 2500° to 3500° F.

Lewis Research Center
National Aeronautics and Space Administration
Cleveland, Ohio, February 18, 1963

REFERENCES

1. Johnson, W. H.: Melting and Casting of the Refractory Metals, Molybdenum, Columbium, Tantalum, and Tungsten. DMIC Rep. 139, Defense Metals Info. Center, Nov. 18, 1960.

2. Torti, M. L.: Arc-Melting Procedures for Refractory Metals. Trans. Vacuum Metallurgy Conf., Rointan F. Bunshah, ed., New York Univ. Press, 1959, pp. 1-4.

3. Morgan, R. P., and Schottmiller, J. C.: The Consolidation and Purification of Tungsten in High Vacuum. Trans. Vacuum Metallurgy Conf., Rointan F. Bunshah, ed., New York Univ. Press, 1959, pp. 5-14.

4. Noesen, S. S., and Parke, R. M.: Consumable Electrode Arc Melting of Refractory Metals. Vacuum Metallurgy, R. F. Bunshah, ed., Reinhold Pub. Corp., 1958, pp. 162-171.

5. Foyle, Fred A.: Arc-Melted Tungsten and Tungsten Alloys. Paper Presented at High-Temperature Materials Conf., AIME, Cleveland (Ohio), Apr. 26-27, 1961.

6. Smith, H. R.: Electron Bombardment Melting Techniques. Vacuum Metallurgy, R. F. Bunshah, ed., Reinhold Pub. Corp., 1958, pp. 221-235.

7. Atkinson, R. H., et al.: Physical Metallurgy of Tungsten and Tungsten Base Alloys. TR 60-37, WADD, May 1960.

8. Carlson, R. G.: Tungsten Zone Melting by Electron Bombardment. Jour. Electrochem. Soc., vol. 106, no. 1, Jan. 1959, pp. 49-52.

9. Witzke, Walter R.: The Purification of Tungsten by Electron-Bombardment Floating-Zone Melting. Trans. Vacuum Metallurgy Conf., Rointan F. Bunshah, ed., New York Univ. Press, 1959, pp. 140-148.

10. Clark, J. W.: Physical Metallurgy of Welding Tungsten and Tungsten-Base Alloys. TR-61-584, Aero. Systems Div., Jan. 1962.

11. Anon.: W-100 - Electron Beam Melted Grain Refined Tungsten. Metals Div., Stauffer Chem. Co., May 1961.

12. Gruber, Helmut: Das Schmelzen von Metallen mit Elektronenstrahlen. (Electron Beam Methods for the Melting of Metals.) Zs. f. Metallkunde, bd. 52, nr. 5, May 1961, pp. 291-309.

13. Gordon, W. A., Tumney, Z. T., and Graab, J. W.: The Conductometric Determination of Carbon Below 10 PPM in Zone-Refined Tungsten. Conf. on Analytical Chem. and Appl. Spectroscopy, Pittsburgh (Pa.), Mar. 5-9, 1962, p. 59.

14. Haymes, J. G., and Ollar, Albert: Methods for Determining Microquantities of Impurities in Tungsten. RI 6005, Bur. Mines, 1962.

15. Foyle, Fred A., McDonald, Glen E., and Saunders, Neal T.: Initial Investigation of Arc Melting and Extrusion of Tungsten. NASA TN D-269, 1960.

16. Sikora, Paul F., and Hall, Robert W.: High-Temperature Tensile Properties of Wrought Sintered Tungsten. NASA TN D-79, 1959.

17. Imgram, Albert G., Holden, Frank C., Ogden, Horace R., and Jaffee, Robert I.: Notch Sensitivity of Refractory Metals. TR 60-278, WADD, Apr. 1960.

18. Orehotsky, J. L., and Steinitz, R.: The Effect of Zone Purification on the Transition Temperature of Polycrystalline Tungsten. Trans. AIME, vol. 224, no. 3, June 1962, pp. 556-560.

19. Hall, Robert W., and Sikora, Paul F.: Tensile Properties of Molybdenum and Tungsten from 2500° to 3700° F. NASA MEMO 3-9-59E, 1959.

20. Staff of Metals Research Laboratories, Union Carbide Co.: Investigation of the Properties of Tungsten and Its Alloys. TR 60-144, WADD, May 1960.

TABLE I. - ELECTRON-BEAM-MELTED INGOT HISTORY

Ingot	Tungsten starting material		Approximate melting rate, lb/hr				
	Diameter, in.	Preparation	Melt 1	Melt 2	Melt 3	Melt 4	Melt 5
EB10	2	Arc melted	7.5	10.5	--	---	--
EB15	1	Sintered	2.9	14.0	16	9.4	25
EB20	1	Sintered	3.6	17.5	--	---	--

TABLE II. - CHEMICAL ANALYSIS OF VARIOUS TUNGSTEN MATERIALS

[<, not detected and therefore less than quantity indicated.]

Element	Impurities, ppm		
	Pressed and sintered tungsten melt stock	Typical arc-melted ingot (average of five single melts)	Electron-beam-melted ingot EB20 (typical double melt)
Aluminum	10	<5	<2
Boron	<2	<3	<2
Cadmium	<10	<10	<10
Chromium	<5	<10	<5
Copper	<1	<3	<1
Iron	10	15	2
Manganese	<1	<5	<1
Molybdenum	<10	10	<10
Sodium	<10	10	<10
Nickel	8	12	<2
Lead	<10	<10	<10
Silicon	10	7	<3
Thorium	<30	<50	<30
Phosphorus	<20	<50	<20
Potassium	<10	<20	<10
Tin	<5	<10	<5
Sulfur	18	15	<10
Oxygen	11	13	3
Hydrogen	<1	<1	<1
Nitrogen	15	18	13
Carbon	8	13	11

TABLE III. - ELECTRON-BEAM-MELTED TUNGSTEN EXTRUSION DATA

Specimen	Billet[a]			Reduction ratio	Extrusion temperature, °F	Extrusion speed, in./sec	Die coating	Lubricant	Extruded product		
	Diameter, in.	Length, in.	Average Vickers hardness (10-kg load)						Average diameter, in.	Total length, in.	Average Vickers hardness (10-kg load)
Dynapak extrusions											
EB10-1	1.65	$2\frac{1}{4}$	357	8	3200	[b]4000	None	None	0.66	$15\frac{3}{4}$	366
EB10-3	1.65	$2\frac{1}{4}$		8	3200		None	Corning 7900 glass	.62	$17\frac{3}{4}$	(c)
EB10-4	[d]1.65	$2\frac{1}{4}$		8	3160		None	Corning 7900 glass[e]	.62	$16\frac{1}{4}$	(c)
EB10-7	1.66	$2\frac{1}{2}$		10	3200		Alumina	Corning 7900 glass[e]	.50	25	366
EB10-8	1.66				3400 to 3500		Alumina	Corning 7900 glass[e]	.54	$21\frac{3}{4}$	(c)
EB20-1	[d]1.70		376		3000		Corning 0010 glass	Corning 7740 glass	.56	$23\frac{7}{8}$	(c)
EB20-2					3000			None	.56	$23\frac{1}{4}$	356
EB20-3				8	[f]2400			Corning 7740 glass[e]	.66	$12\frac{1}{2}$	345
EB20-4				8	3000			Corning 7740 glass[e]	.65	$19\frac{1}{4}$	357
Hydraulic-press extrusion											
EB15	2.060	$4\frac{1}{2}$	383	8	3150	5.9	Alumina	Corning 7740 glass	0.77	$32\frac{1}{8}$	360

[a]All billets had 120° included angle on nose end.

[b]Estimated.

[c]Not determined.

[d]Brass sheet (0.008 in.) used in container.

[e]Copper nose pad used ahead of billet.

[f]Estimated. Water leak quenched billet.

TABLE IV. - MECHANICAL PROPERTIES OF EXTRUDED ELECTRON-BEAM-MELTED TUNGSTEN

Extrusion billet	Test temperature, °F	Ultimate tensile strength, psi	0.2-Percent yield strength, psi	Reduction in area, percent	Uniform elongation, percent	Total elongation, percent
EB10-8	70	(a)	(a)	(a)	(a)	(a)
EB10-4	70	(a)	(a)	(a)	(a)	(a)
EB10-4	390	25,800	(b)	0	0	0
EB10-3	505	24,800	(b)	0	0	0
EB10-1	515	55,800	29,900	9	6.9	8.2
EB10-3	710	39,500	16,700	11	9.6	9.8
EB10-7	900	33,100	13,100	7	6.9	6.9
EB10-8	980	39,700	9,700	(c)	34.6	34.6
EB10-7	1095	37,500	12,450	69	29.5	39.2
EB10-1	1200	36,500	11,050	97	33.6	43.7
EB10-8	1305	31,900	10,500	94	31.4	44.5
EB10-4	1500	30,900	11,800	95	38.8	51.7
EB10-3	2000	24,900	5,700	99	37.3	57.3
EB10-1	2000	25,600	4,800	99	36.4	55.2
EB10-8	2500	18,000	4,300	99	29.7	59.0
EB10-7	2500	18,000	4,300	99	28.4	57.0
EB10-7	3000	15,100	4,800	99	22.3	57.9
EB10-8	3000	12,700	3,800	99	18.8	53.4
EB10-3	3500	7,500	-----	99	17.3	62.7
EB10-1	3500	6,600	800	99	16.4	47.9
EB10-8	3900	4,300	970	99	13.8	47.5
EB10-4	3900	4,000	430	99	14.2	77.5
EB10-7	3900	4,900	710	99	11.1	62.5
EB10-3 (swaged)	795	60,100	56,500	66	2.8	11.8
EB15	70	30,000	(a)	(a)	(a)	(a)
EB15	70	39,000	(a)	(a)	(a)	(a)
EB15	500	55,200	37,600	0	2.0	2.0
EB15	700	45,900	15,100	16	14.9	14.9
EB15	900	43,200	12,800	86	34.0	48.4
EB15	1500	31,700	8,900	99	37.6	62.9
EB15	2000	25,300	4,400	99	34.5	55.2
EB15	2500	18,800	3,900	99	29.6	49.3
EB15	3000	12,300	1,500	99	21.0	37.6
EB15	3500	8,000	1,200	99	17.7	52.4
EB15	3900	4,600	990	99	14.9	58.6
EB15 (swaged)	535	93,700	83,700	59	3.9	10.7
EB15 (swaged)	585	90,400	83,500	65	3.9	16.2
EB15 (swaged)	670	52,100	42,400	77	15.4	25.8
EB15 (swaged)	2500	18,600	6,700	99	36.0	48.6
EB15 (swaged)	3500	7,200	1,150	99	16.8	55.3
EB20-2	880	35,100	13,800	5	4.7	6.2
EB20-4	975	40,000	15,200	76	25.4	35.4
EB20-2	1100	38,400	11,700	92	32.2	44
EB20-2	1500	29,500	------	94	43.0	55
EB20-4	1600	29,600	11,150	94	40.0	56
EB20-4	2000	22,400	7,450	99	37.2	45
EB20-2	2500	18,100	6,440	(d)	21.5	(d)
EB20-4	3000	11,400	3,290	99	21.2	64
EB20-2	3020	13,000	1,730	99	19.0	51
EB20-2	3500	7,890	1,430	99	14.1	37.6
EB20-4	3500	6,360	2,010	(a)	15.5	(a)
EB20-4	3900	4,320	1,070	(a)	6.8	(a)
EB20 (swaged)	715	63,800	60,800	68	2.7	12.3
EB20 (swaged)	3000	11,100	------	99	20.6	39.2

[a]Broke or cracked in fillet.

[b]Broke before yield.

[c]Broke in midsection and fillet.

[d]Circumferential crack prior to necking.

TABLE V. - MECHANICAL PROPERTIES OF RECRYSTALLIZED POWDER METALLURGY TUNGSTEN

Test temperature, °F	Ultimate tensile strength, psi	0.2-Percent yield strength, psi	Reduction in area, percent	Uniform elongation, percent	Total elongation, percent
575	64,400	18,950	13	16.7	----
640	62,600	19,290	65	29.7	39.4
700	59,200	13,750	69	31.5	45
1030	46,500	18,300	84	34.5	50.9
2000	30,600	10,700	99	29.5	45.4
2500	22,200	5,200	99	19.3	28.8
3000	15,200	4,050	81	18.4	42.1
3500	10,100	3,650	46	14.9	42.3
3500	9,930	2,900	40	16.8	44.2

TABLE VI. - RECRYSTALLIZATION OF EXTRUDED AND SWAGED ELECTRON-BEAM-MELTED TUNGSTEN

Temperature[a], °F	Average Vickers hardness (10-kg load)	Observed recrystallization, percent
As swaged[b]	437	--
2000	417	35
2170	354	85
2250	336	95
2500	339	100
3000	333	100

[a]1 hr annealing temperature.

[b]Extrusion of ingot EB15 swaged to 70-percent reduction in area at 2200° to 2400° F.

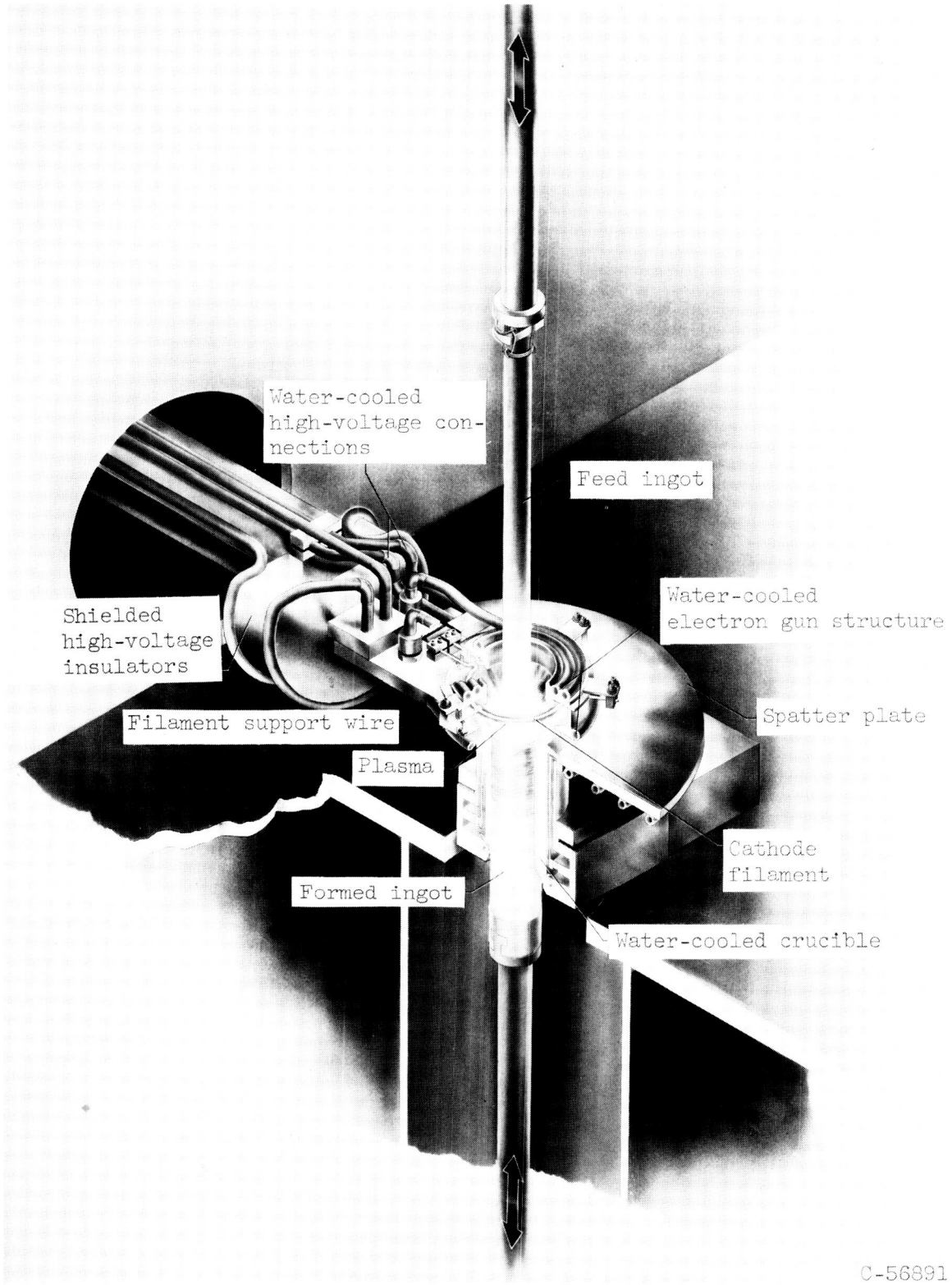

Figure 1. - Melting equipment in electron-beam furnace.

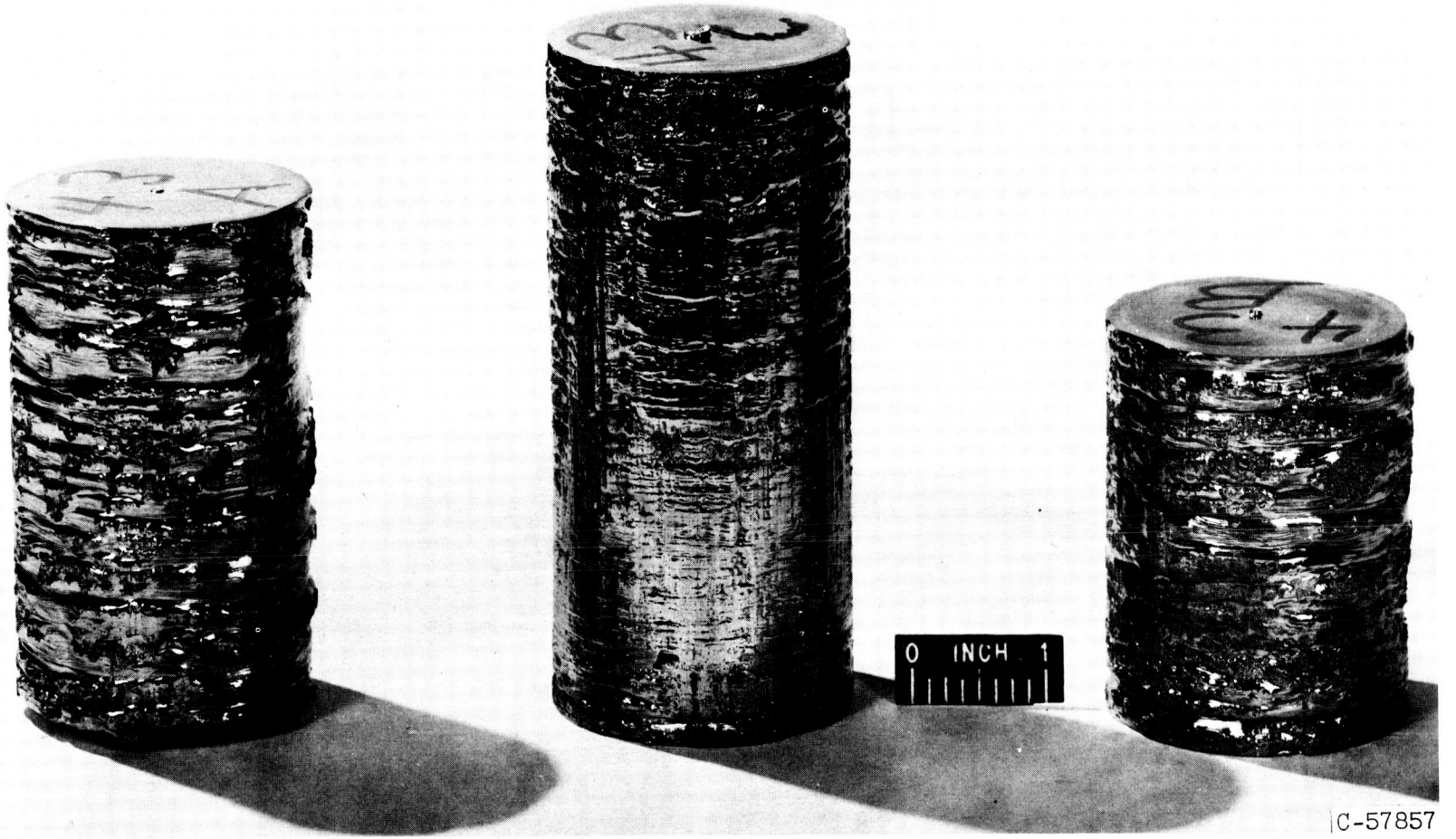

(a) Sections of tungsten ingot.

Figure 2. - Representative surfaces of electron-beam-melted ingots.

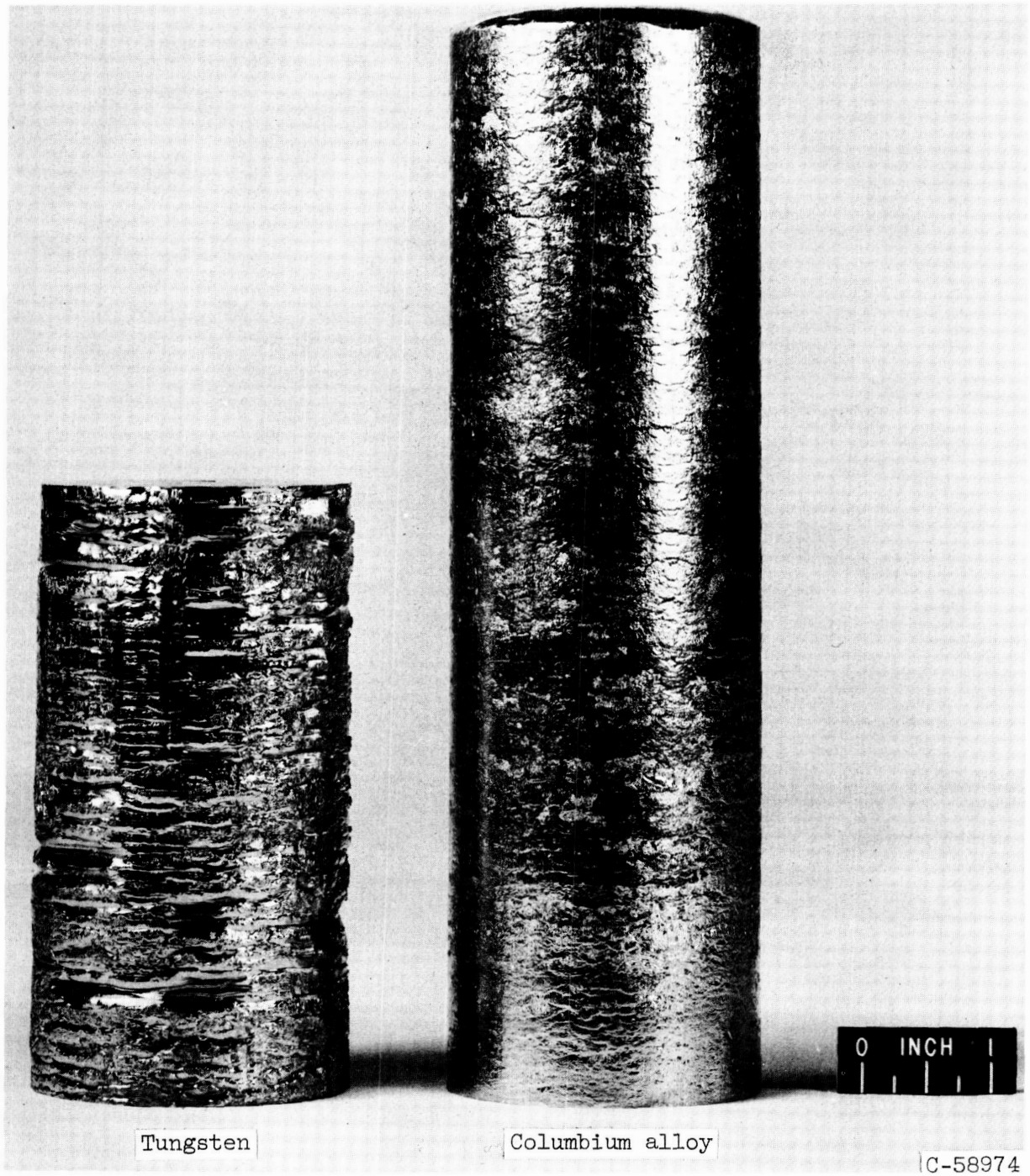

(b) Comparison of tungsten and columbium-alloy ingots.

Figure 2. - Concluded. Representative surfaces of electron-beam-melted ingots.

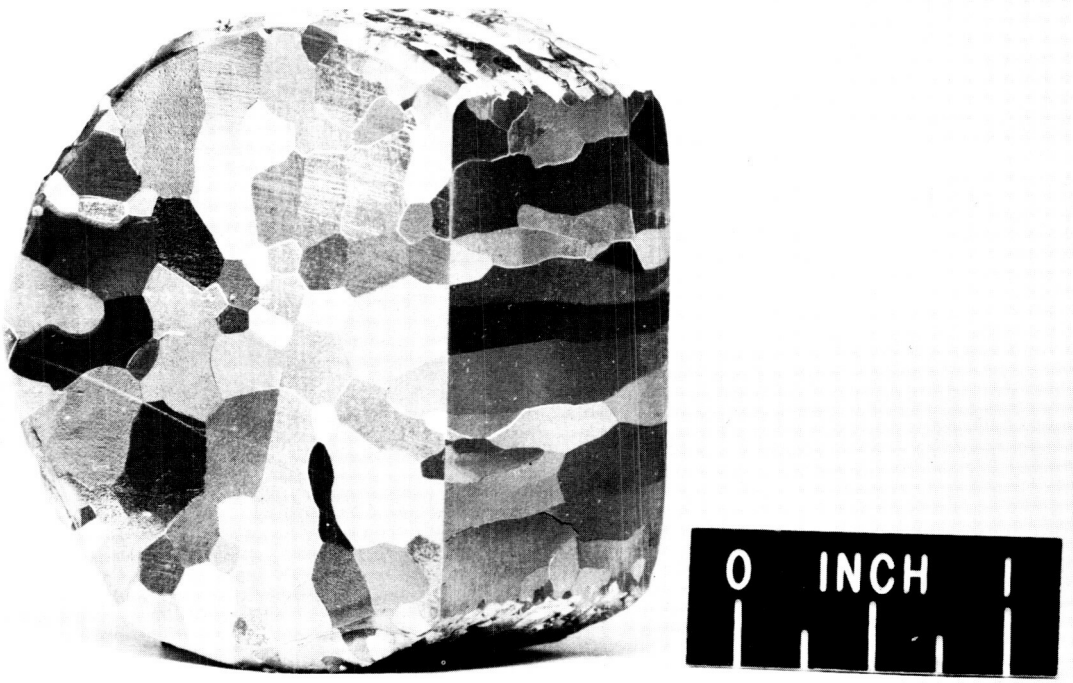

C-58786

Figure 3. - Columnar grains in electron-beam-melted tungsten ingot.

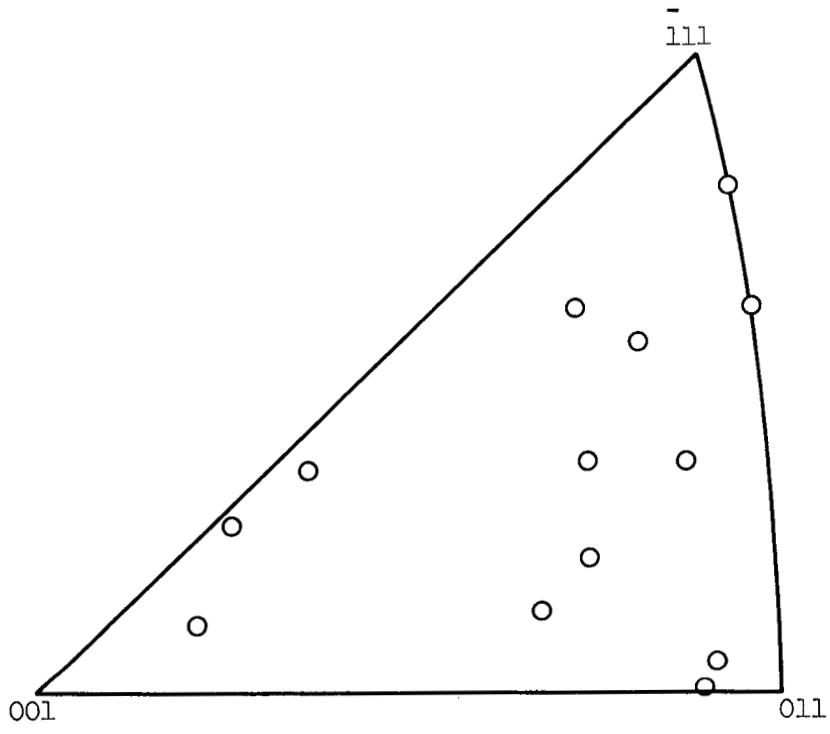

Figure 4. - Orientation of individual grains in several electron-beam-melted ingots.

Figure 5. - Intergranular fracture of electron-beam-melted tungsten. Etchant, potassium hydroxide plus potassium ferricyanide.

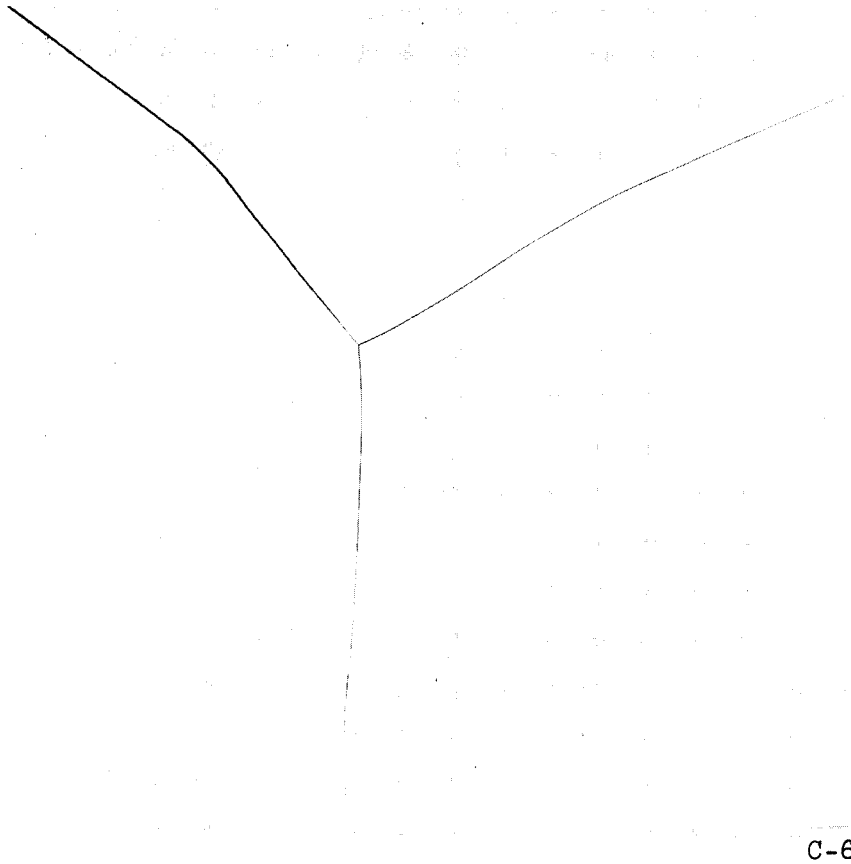

C-61784

Figure 6. - Photomicrograph of electron-beam-melted tungsten. Etchant, potassium hydroxide plus potassium ferricyanide; X250.

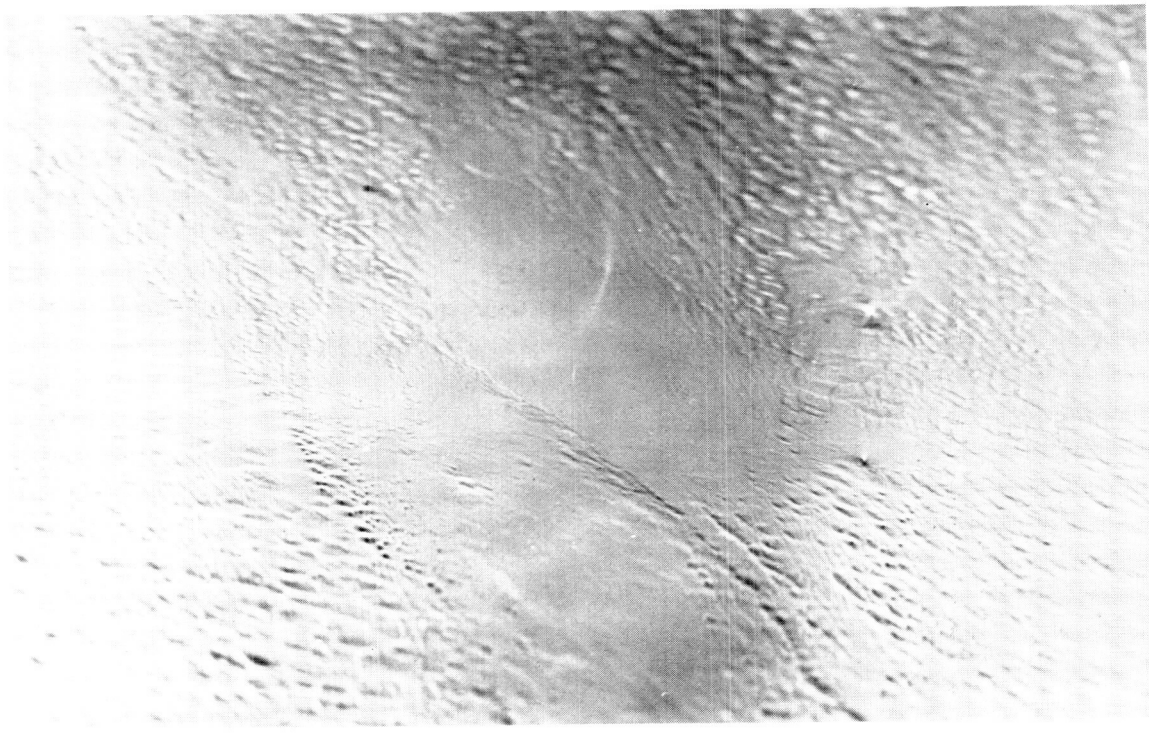

(a) Tungsten ingot EB10.

(b) Tungsten ingot EB20.

Figure 7. - Typical fractographs of electron-beam-melted tungsten ingots. ×200 (reduced 7 percent in printing).

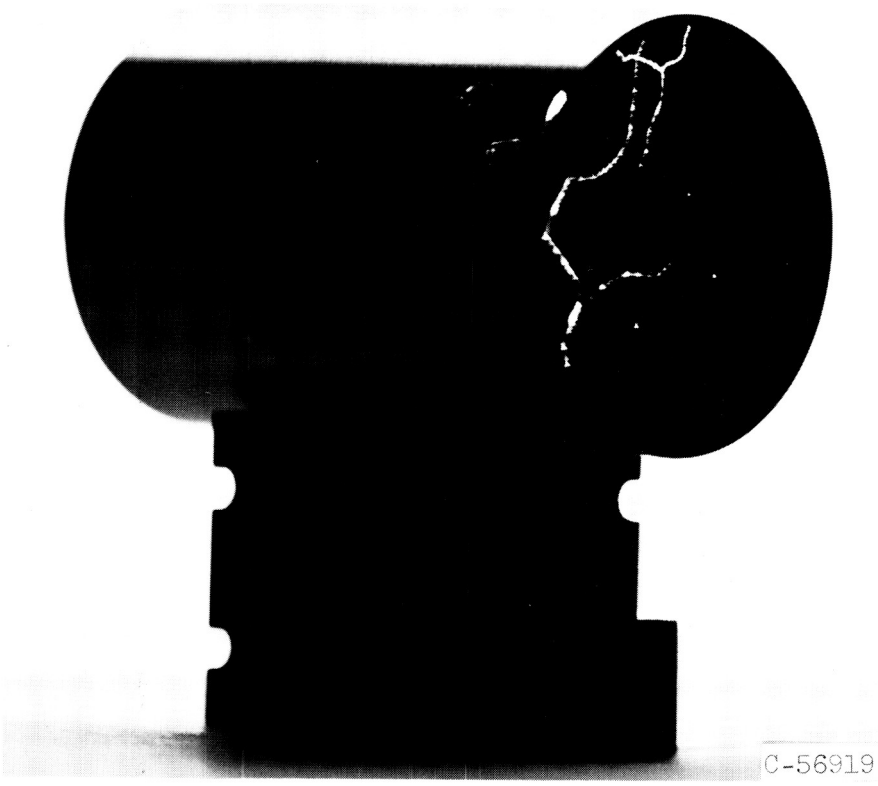

Figure 8. - Ultraviolet photograph of electron-beam-melted tungsten extrusion billet.

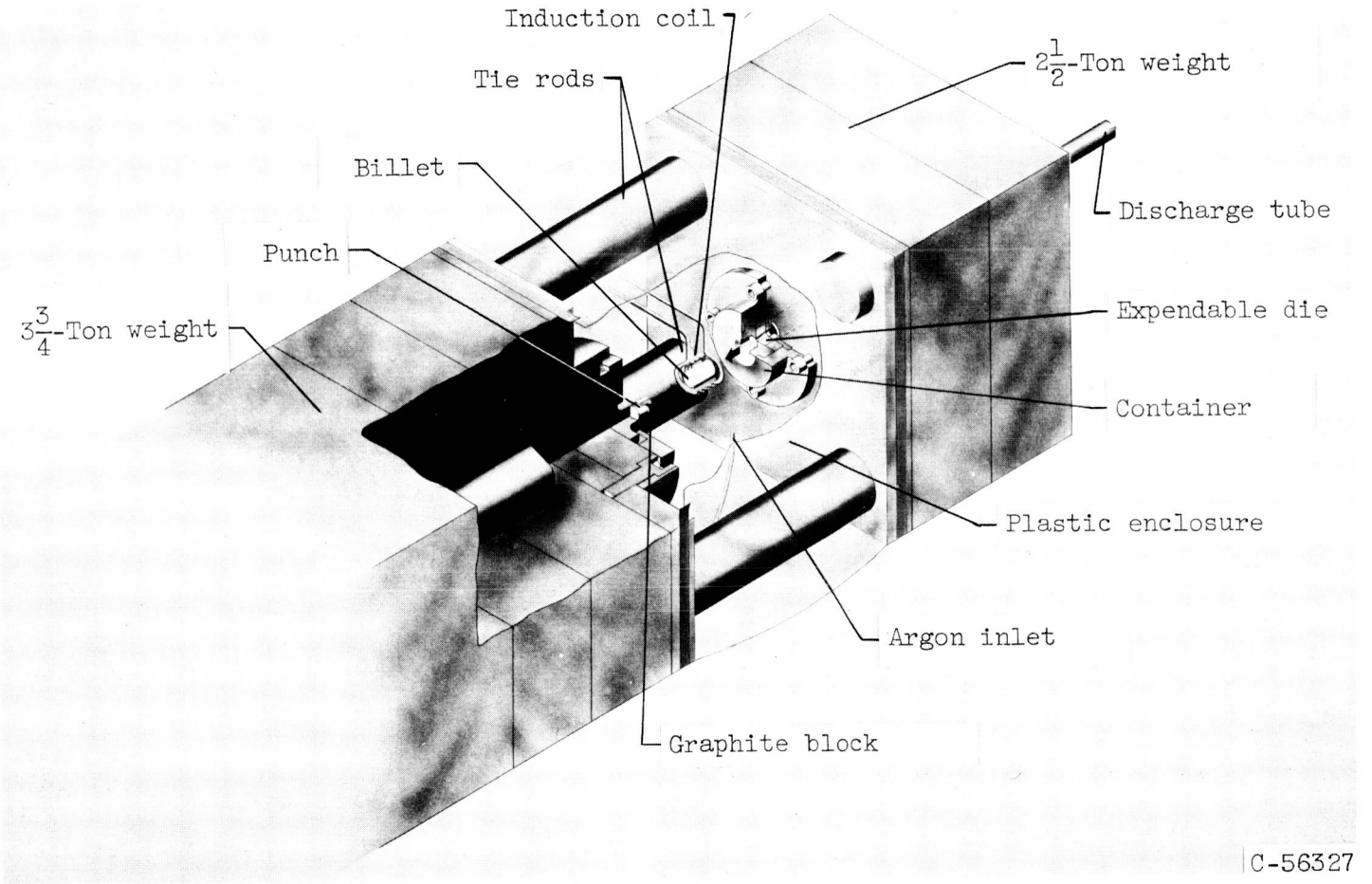

Figure 9. - Dynapak high-velocity extrusion press.

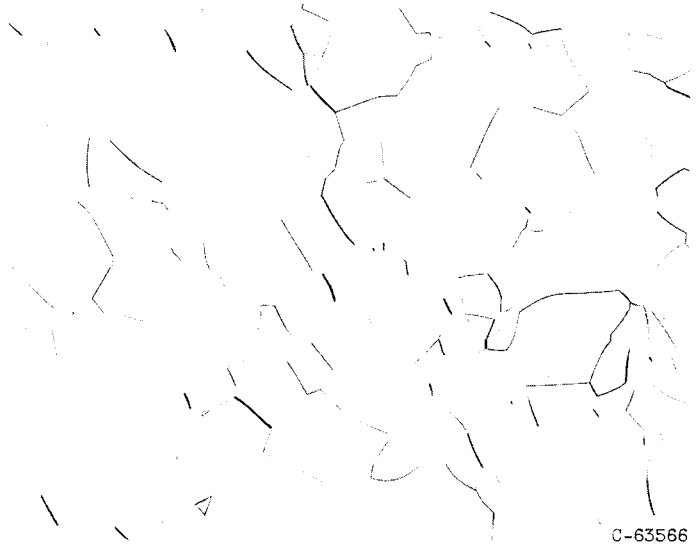

C-63566

(a) Tungsten billet EB10-1. Dynapak extrusion.

C-63567

(b) Tungsten billet EB15. Hydraulic-press extrusion.

C-63568

(c) Tungsten billet EB20-2. Dynapak extrusion.

Figure 10. - Typical microstructures of as-extruded electron-beam-melted tungsten. Etchant, potassium hydroxide plus potassium ferricyanide; ×250 (reduced 32 percent in printing).

(a) Reduction ratio, 8.

Figure 11. - Extrusions of tungsten produced on Dynapak press.

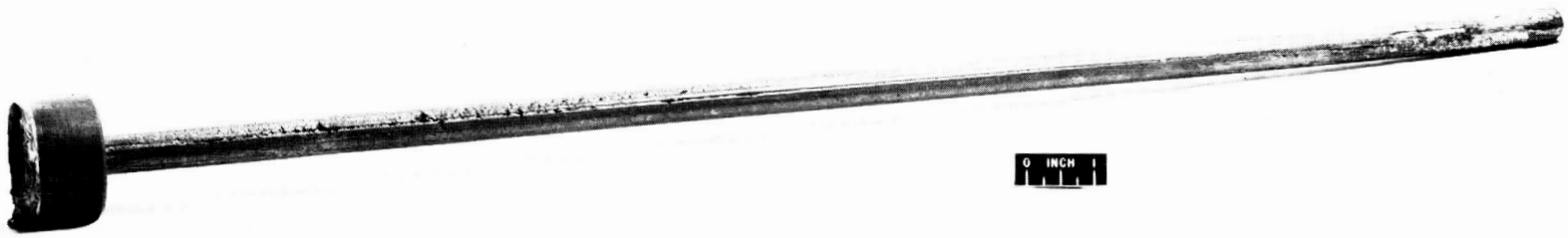

C-57729

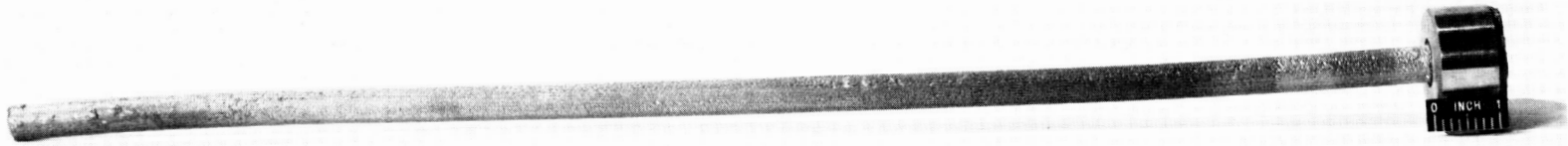

C-57833

(b) Reduction ratio, 10.

Figure 11. - Concluded. Extrusions of tungsten produced on Dynapak press.

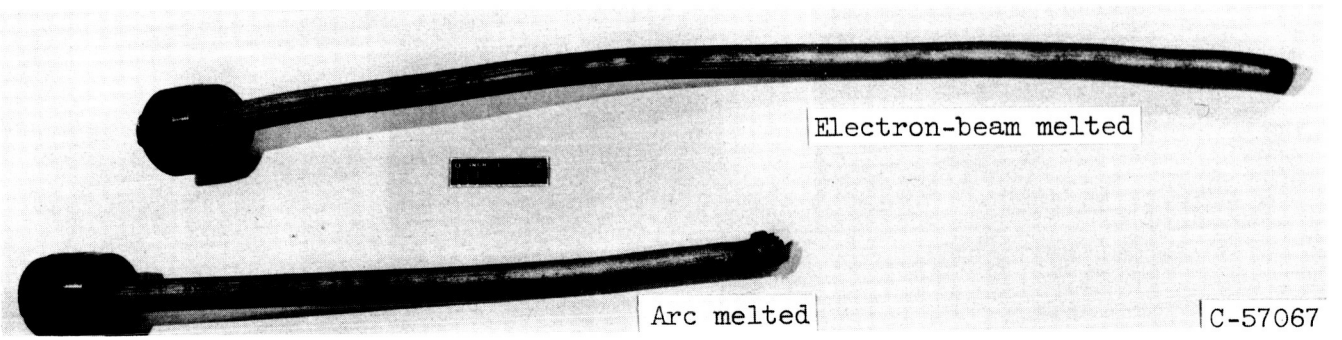

Figure 12. - Extrusions of tungsten produced on hydraulic press.

Figure 13. - Microstructure of tungsten extrusion EB15 as swaged. Etchant, potassium hydroxide plus potassium ferricyanide; ×100.

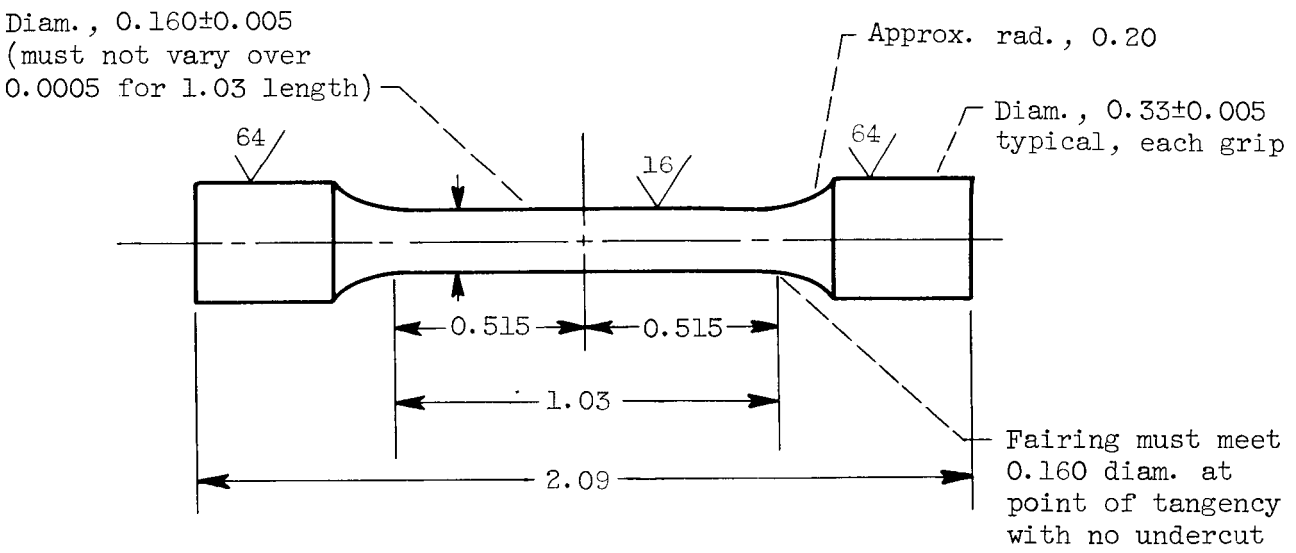

Figure 14. - Tensile specimens. (All dimensions in inches.)

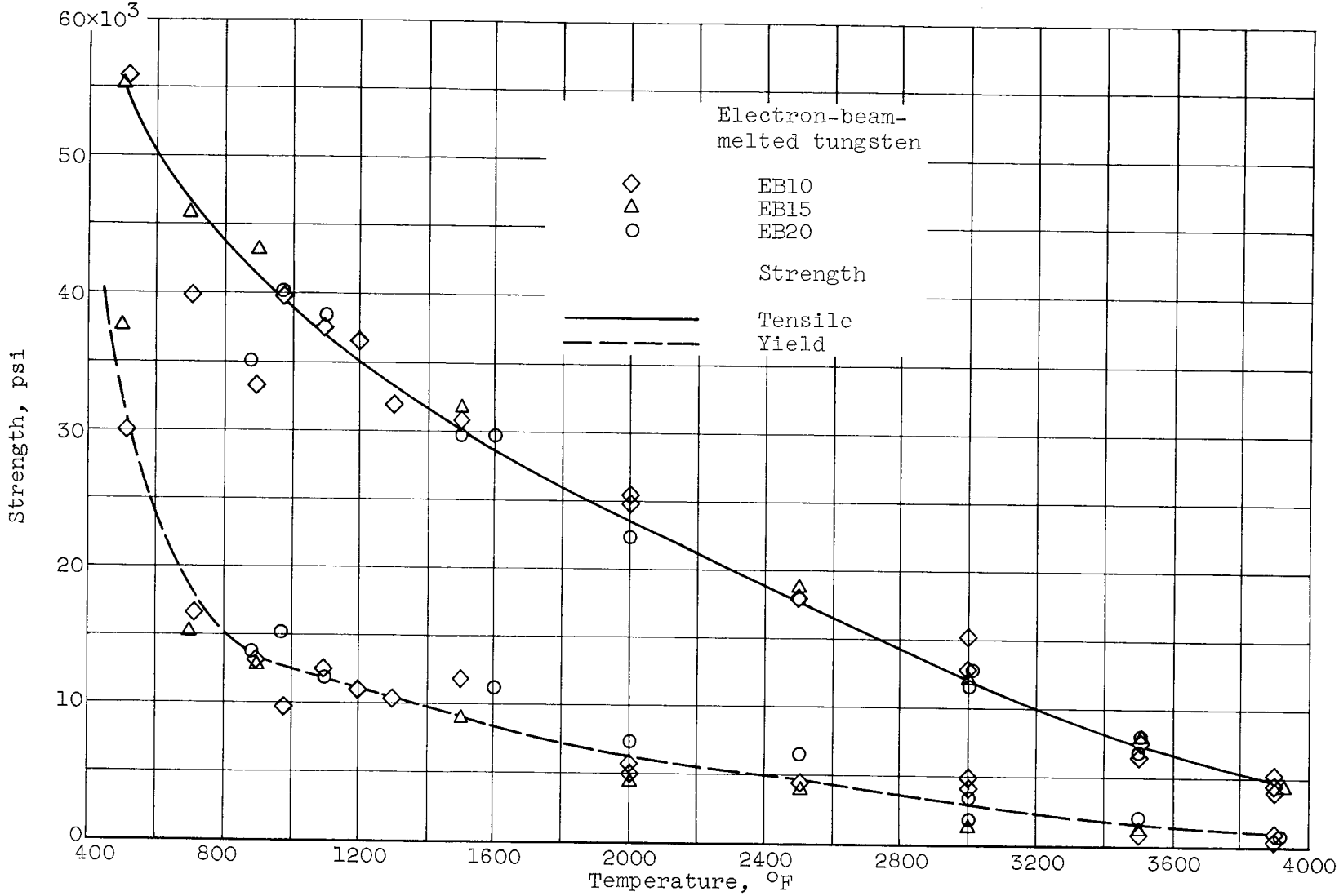

Figure 15. - Strength properties of extruded electron-beam-melted tungsten as function of temperature.

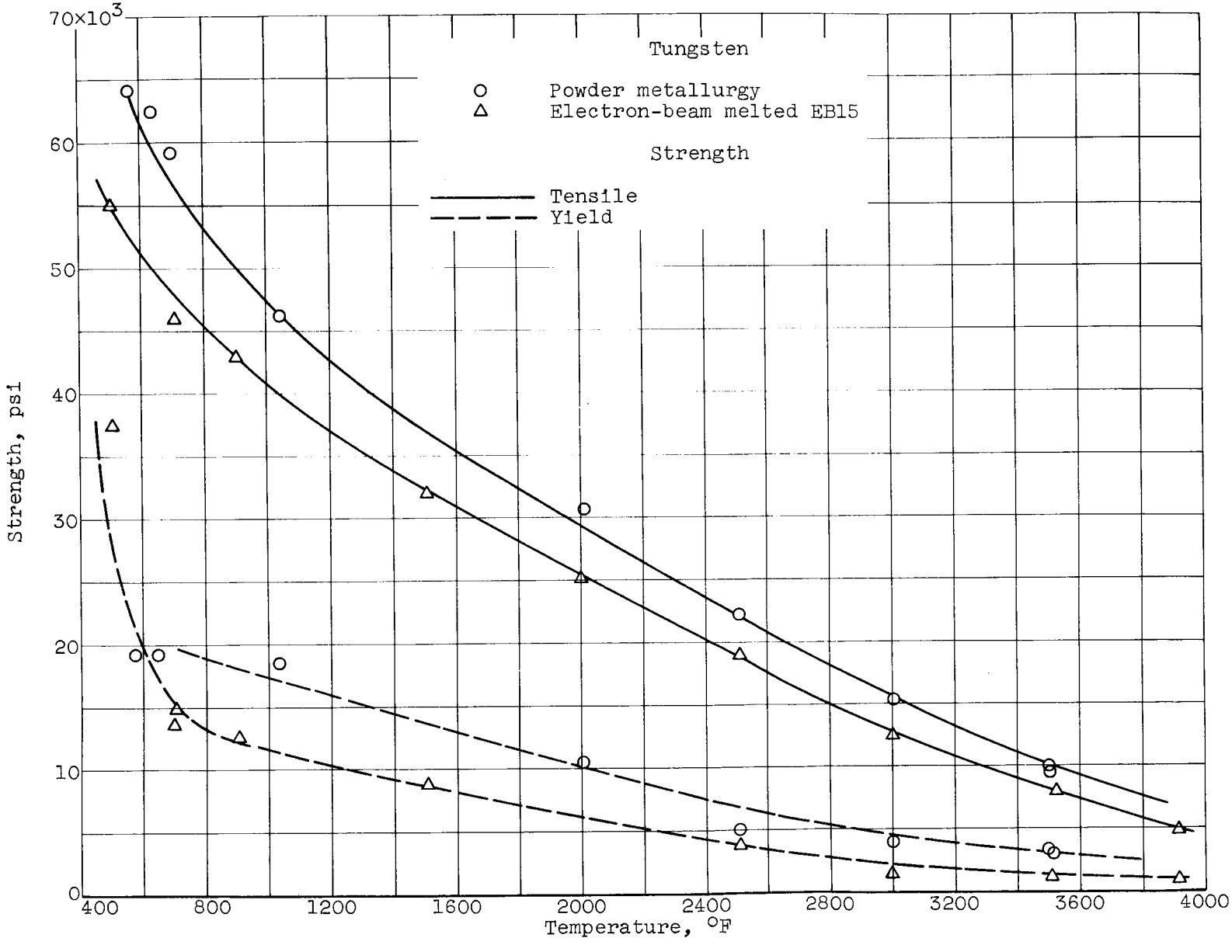

Figure 16. - Comparative strength of extruded electron-beam-melted and powder metallurgy tungsten as function of temperature for material of equal grain size.

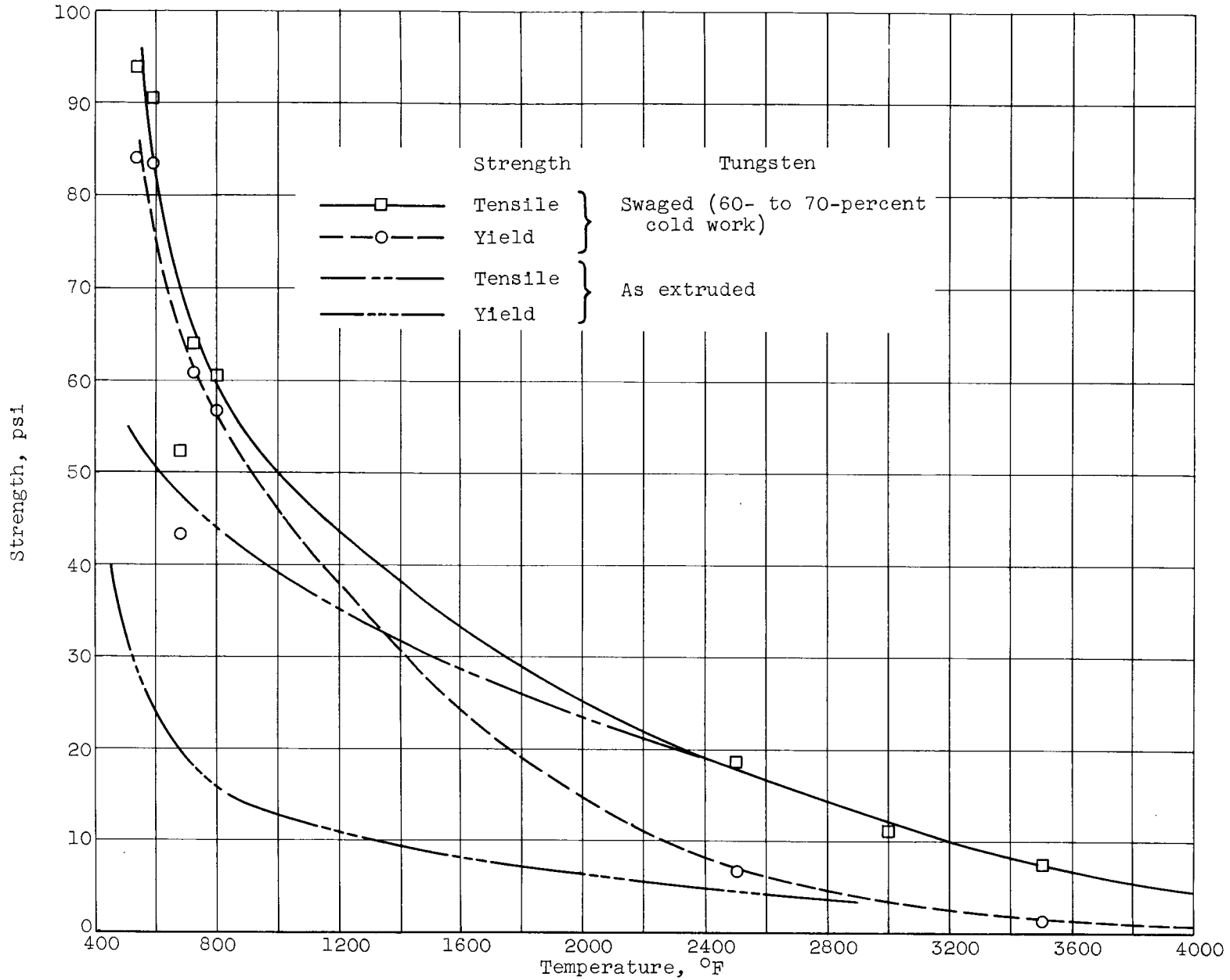

Figure 17. - Effect of cold work on strength properties of electron-beam-melted tungsten.

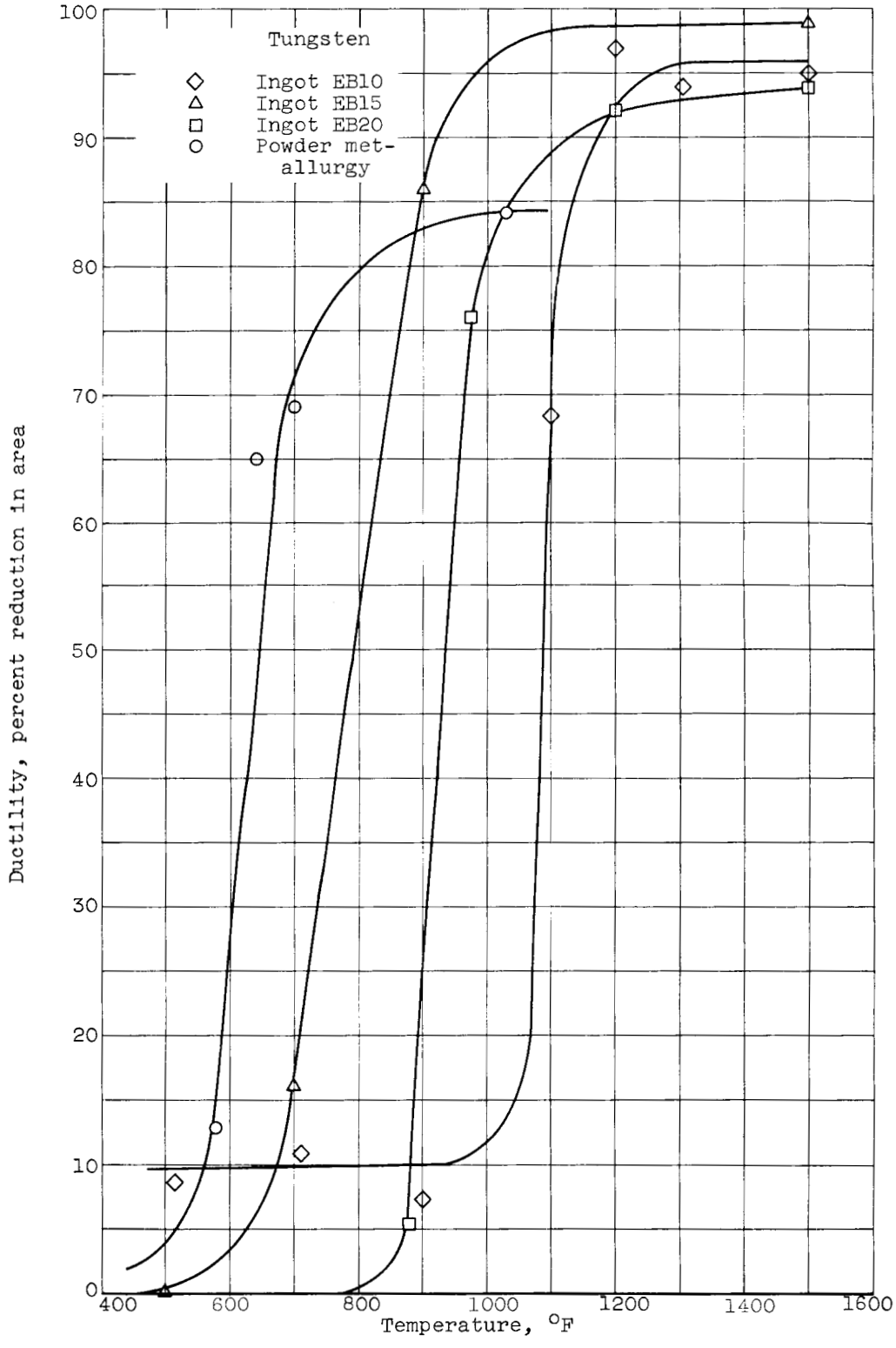

Figure 18. - Ductile-to-brittle transition temperature for extruded electron-beam-melted tungsten and swaged powder metallurgy tungsten.

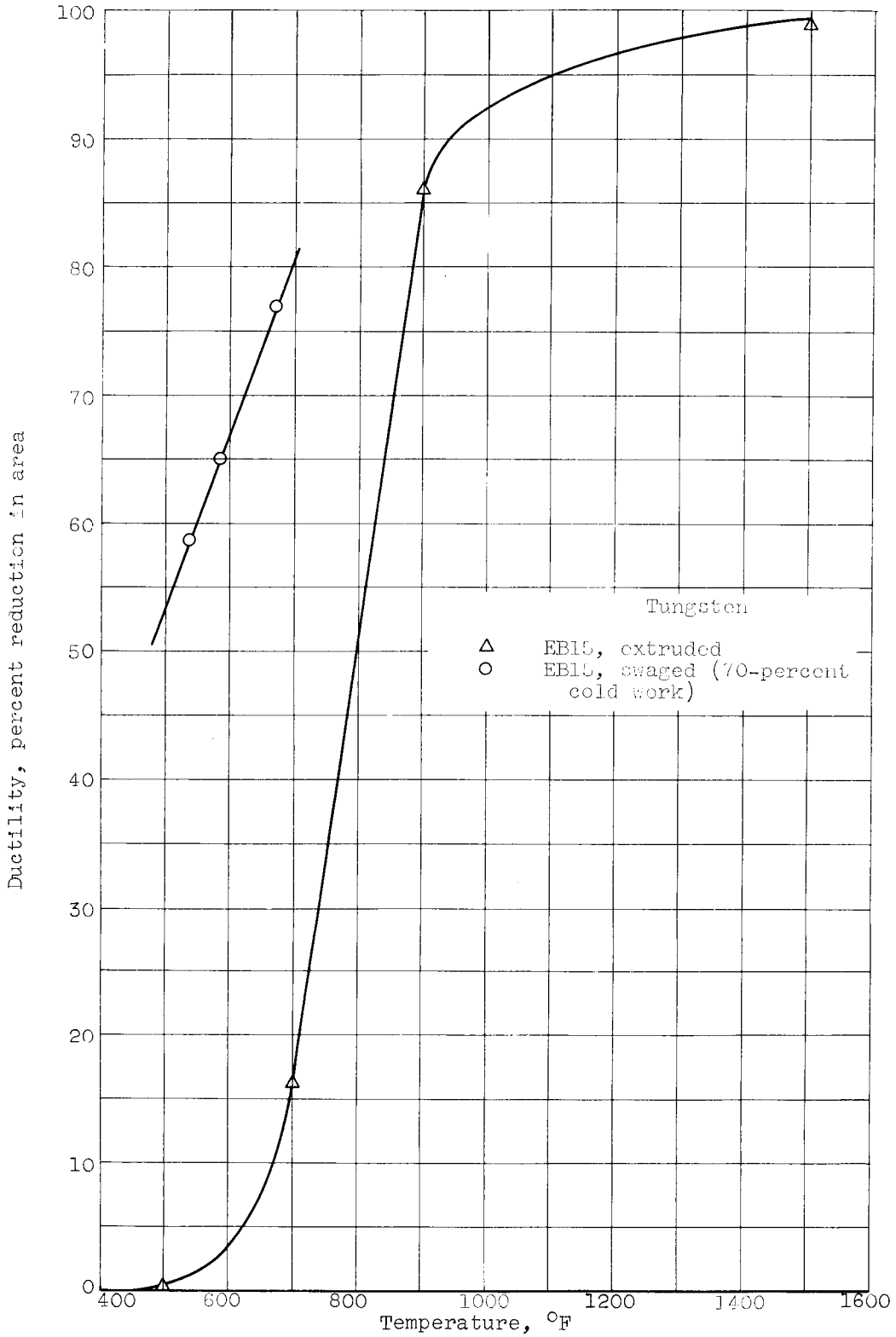

Figure 19. - Ductile-to-brittle transition temperature for swaged and extruded electron-beam-melted tungsten.

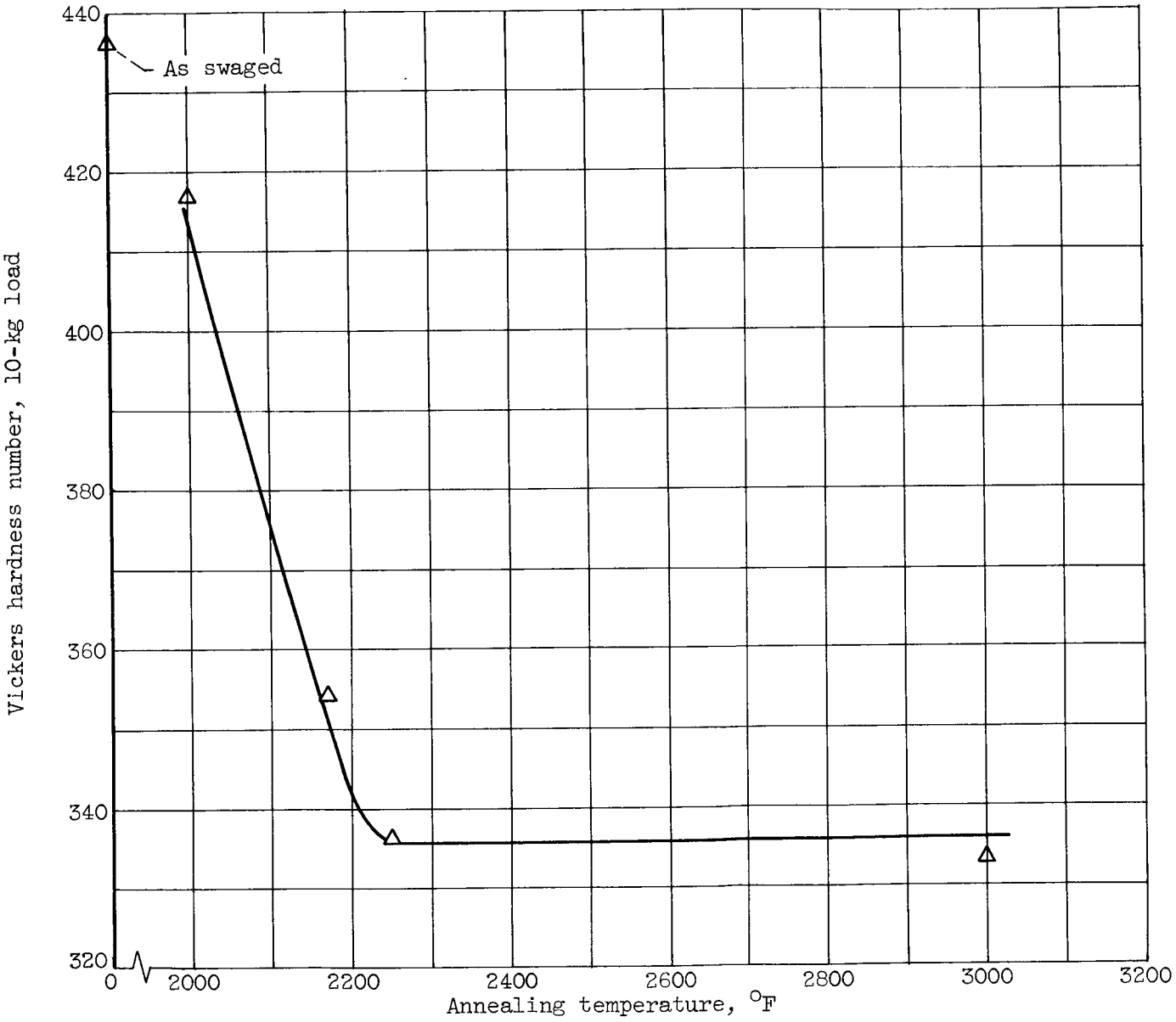

Figure 20. - Effect of annealing temperature on hardness of swaged electron-beam-melted tungsten EB15. Annealing time, 1 hour.

(a) Temperature, 505° F.

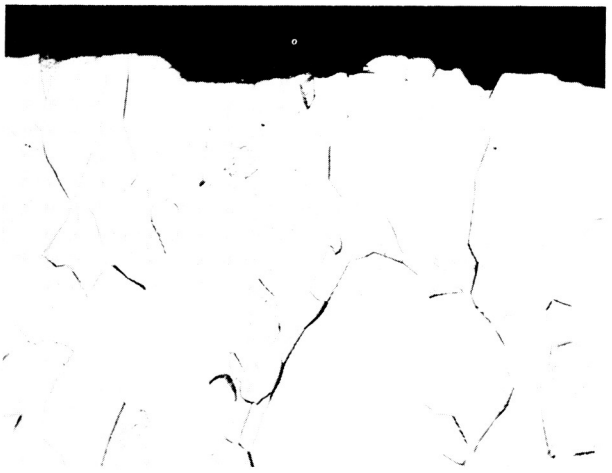

(b) Temperature, 980° F.

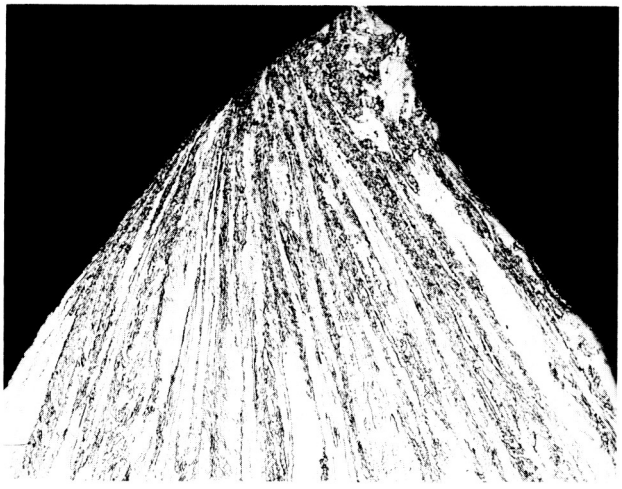

(c) Temperature, 2000° F.

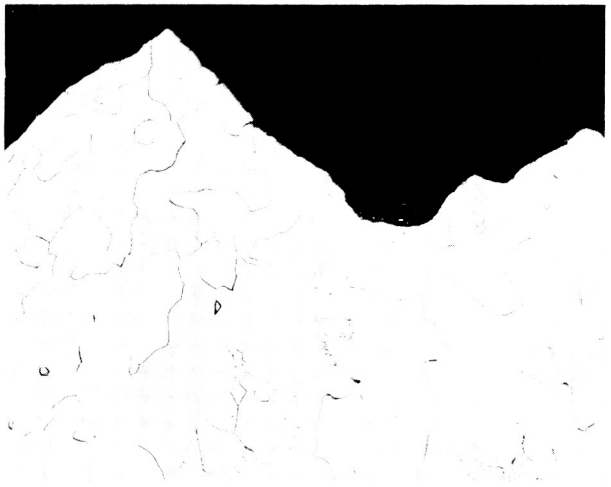

(d) Temperature, 2500° F.

(e) Temperature, 3000° F.

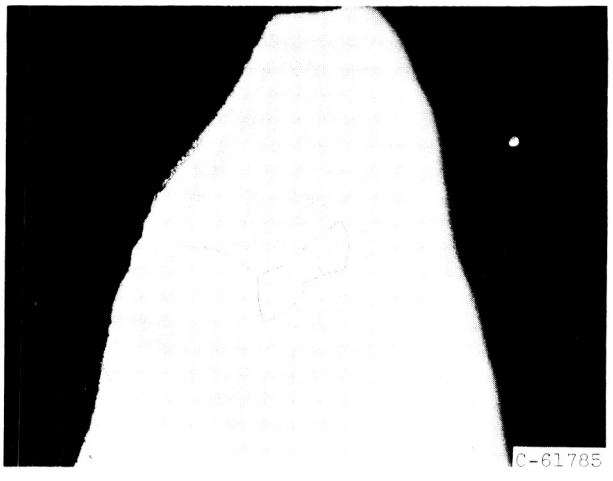

(f) Temperature, 3500° F.

Figure 21. - Fractures of electron-beam-melted tungsten EB10 tested at designated temperatures. Etchant, potassium hydroxide plus potassium ferricyanide; ×100 (reduced 35 percent in printing).